Mon. Not. R. Astron. Soc. **000**, 000–000 (0000) Printed 28 May 2018 (MN LATEX style file v2.2)

A submillimetre galaxy at $z = 4.76$ in the LABOCA survey of the Extended Chandra Deep Field South

K. E. K. Coppin,[1] Ian Smail,[1] D. M. Alexander,[2] A. Weiss,[3] F. Walter,[4] A. M. Swinbank,[1] T. R. Greve,[4] A. Kovacs,[3] C. De Breuck,[5] M. Dickinson,[6] E. Ibar,[7] R. J. Ivison,[7,8] N. Reddy,[6] H. Spinrad,[9] D. Stern,[10] W. N. Brandt,[11] S. C. Chapman,[12] H. Dannerbauer,[4] P. van Dokkum,[14] J. S. Dunlop,[7] D. Frayer[13] E. Gawiser,[15] J. E. Geach,[1] M. Huynh,[13] K. K. Knudsen,[16] A. M. Koekemoer,[17] B. D. Lehmer,[2] K. M. Menten,[3] C. Papovich,[18] H.-W. Rix,[4] E. Schinnerer,[4] J. L. Wardlow,[2] P. P. van der Werf[19]

[1] *Institute for Computational Cosmology, Durham University, South Road, Durham, DH1 3LE, UK*
[2] *Department of Physics, Durham University, South Road, Durham, DH1 3LE, UK*
[3] *Max-Planck-Institut für Radioastronomie, Auf dem Hügel 69, Bonn, D-53121, Germany*
[4] *Max-Planck-Institut für Astronomie, Königstuhl 17, Heidelberg, D-69117, Germany*
[5] *European Southern Observatory, Karl-Schwarzschild Strasse, 85748 Garching bei München, Germany*
[6] *National Optical Astronomy Observatory, P.O. Box 26732, Tucson, AZ 85726, USA*
[7] *SUPA⋆, Institute for Astronomy, University of Edinburgh, Royal Observatory, Blackford Hill, Edinburgh, EH9 3HJ, UK*
[8] *UK Astronomy Technology Centre, Royal Observatory, Blackford Hill, Edinburgh, EH9 3HJ, UK*
[9] *Department of Astronomy, University of California at Berkeley, Mail Code 3411, Berkeley, CA 94720, USA*
[10] *Jet Propulsion Laboratory, California Institute of Technology, Mail Stop 169-527, Pasadena, CA 91109, USA*
[11] *Department of Astronomy and Astrophysics, 525 Davey Lab, Pennsylvania State University, University Park, PA 16802, USA*
[12] *Institute of Astronomy, Madingley Road, Cambridge, CB3 0HA, UK*
[13] *Infrared Processing and Analysis Center, MS220-6, California Institute of Technology, Pasadena, CA 91125, USA*
[14] *Department of Astronomy, Yale University, PO Box 208101, New Haven, CT 06520 USA*
[15] *Physics & Astronomy Department, Rutgers University, Piscataway, NJ 08854, USA*
[16] *Argelander Institute for Astronomy, University of Bonn, Auf dem Hügel 71, D-53121 Bonn, Germany*
[17] *Space Telescope Science Institute, 3700 San Martin Drive, Baltimore, MD 21218, USA*
[18] *G.P. & C.M. Mitchell Institute for Fundamental Physics, Department of Physics, Texas A&M University, College Station, TX 77843, USA*
[19] *Leiden Observatory, Leiden University, PO Box 9513, NL-2300 RA Leiden, the Netherlands*

28 May 2018

ABSTRACT

We report on the identification of the highest redshift submillimetre-selected source currently known: LESS J033229.4−275619. This source was detected in the Large Apex BOlometer CAmera (LABOCA) Extended Chandra Deep Field South (ECDFS) Submillimetre Survey (LESS), a sensitive 870-μm survey ($\sigma_{870\mu m} \sim 1.2$ mJy) of the full $30' \times 30'$ ECDFS with the LABOCA camera on the Atacama Pathfinder EXperiment (APEX) telescope. The submillimetre emission is identified with a radio counterpart for which optical spectroscopy provides a redshift of $z = 4.76$. We show that the bolometric emission is dominated by a starburst with a star formation rate of $\sim 1000\,M_{\odot}\,\mathrm{yr}^{-1}$, although we also identify a moderate luminosity Active Galactic Nucleus (AGN) in this galaxy. Thus it has characteristics similar to those of $z \sim 2$ submillimetre galaxies (SMGs), with a mix of starburst and obscured AGN signatures. This demonstrates that ultraluminous starburst activity is not just restricted to the hosts of the most luminous (and hence rare) QSOs at $z \sim 5$, but was also occurring in less extreme galaxies at a time when the Universe was less than 10 per cent of its current age. Assuming that we are seeing the major phase of star formation in this galaxy, then we demonstrate that it would be identified as a luminous distant red galaxy at $z \sim 3$ and that the current estimate of the space density of $z > 4$ SMGs is only sufficient to produce $\gtrsim 10$ per cent of the luminous red galaxy population at these early times. However, this leaves open the possibility that some of these galaxies formed through less intense, but more extended star formation events. If the progenitors of all of the luminous red galaxies at $z \sim 3$ go through an ultraluminous starburst at $z \gtrsim 4$ then the required volume density of $z > 4$ SMGs will exceed that predicted by current galaxy formation models by more than an order of magnitude.

Key words: galaxies: high-redshift – galaxies: evolution – galaxies: formation – submillimetre – galaxies: individual LESS J033229.4−275619, GDS J033229.29−275619.5

1 INTRODUCTION

It is now well established that a significant population of luminous red galaxies exist out to at least $z \sim 1.5$–2 and it has been claimed that most of these are massive and that some of them are old ($> 10^{11}\,\mathrm{M}_\odot$, $\gtrsim 2\,\mathrm{Gyr}$) galaxies (Cimatti et al. 2004; Daddi et al. 2005; Kong et al. 2006; McGrath, Stockton & Canalizo 2007; Hartley et al. 2008). There are indications that many of these massive galaxies were largely formed at earlier times, $z \sim 2.5$–3.5, with a fraction of them already having red colours, suggesting an aging stellar population (Marchesini et al. 2007; Marchesini et al. 2009). If correct, this suggests that these galaxies must have formed the bulk of their stellar populations at $z > 4$ (Daddi et al. 2005; Cimatti et al. 2008; Stockton et al. 2008). The implied star formation rates (SFRs) for these progenitors would then be $\sim 10^2$–$10^3\,\mathrm{M}_\odot\,\mathrm{yr}^{-1}$ and if such vigorous activity occurred in a single halo, it is likely that these systems would appear as ultraluminous infrared galaxies (ULIRGs), whose redshifted far-infrared emission would make them bright submillimetre galaxies (SMGs). However, the confirmation of large numbers of galaxies forming stars at a rate of $\sim 10^3\,\mathrm{M}_\odot\,\mathrm{yr}^{-1}$ at such high redshifts could pose a serious challenge to current hierarchical models, which predict a $z > 4$ SMG surface density about an order of magnitude less ($\sim 10\,\mathrm{deg}^{-2}$) than would be implied if all massive high-redshift galaxies form through this process (e.g. Granato et al. 2004; Baugh et al. 2005; Hopkins et al. 2005; Bower et al. 2006; Swinbank et al. 2008).

Due to the negative K-correction, SMGs can essentially be detected out to $z \sim 8$ (see Blain et al. 2002), but the confirmation of SMGs (if they exist) at these redshifts poses a challenge. The large beamsize of submm cameras (e.g. full width at half maximum (FWHM) $\sim 19''$ for LABOCA) precludes the determination of precise positions for large samples of SMGs without very significant investment in sub-/millimetre interferometry (e.g. Downes et al. 1999; Gear et al. 2000; Dannerbauer et al. 2002, 2008; Wang et al. 2007; Younger et al. 2007, 2008). This makes determining their nature through multiwavelength avenues extremely challenging, since there are typically many objects within this large beam that could be the source of the submillimetre emission. The most successful route to identifying the counterparts of SMGs has been to search for 1.4-GHz counterparts (e.g. Ivison et al. 2002), exploiting the well-known far-infrared–radio correlation (Condon 1992; Helou & Bicay 1993). With deep, $\lesssim 10\,\mu\mathrm{Jy}$ rms, radio maps this provides precise positions for about 60 per cent of the SMG population ($S_{850} \gtrsim 4\,\mathrm{mJy}$), allowing follow-up spectroscopy and yielding a redshift distribution for radio-identified SMGs peaking at $z \sim 2.2$ (Chapman et al. 2005). With the advent of *Spitzer*, a similar approach has exploited $24\,\mu\mathrm{m}$ counterparts to SMGs, when radio counterparts were unavailable, increasing the fraction of identified SMGs to $\gtrsim 70$ per cent (e.g. Ivison et al. 2004, 2007; Pope et al. 2006). Unfortunately the radio and mid-infrared emission dim significantly with redshift, which means that the question of whether a significant proportion of SMGs lie at $z \gtrsim 4$ remains open.

Luminous submillimetre-emitting sources are of course known at $z \sim 4$–6 (e.g. McMahon et al. 1994; Omont et al. 1996; Ivison et al. 1998b; Carilli et al. 2000, 2001; Archibald et al. 2001; Priddey, Ivison & Isaak 2008), but these are all associated with rare and extreme Active Galactic Nuclei (AGN) whose space densities are so low that they are probably not a significant progenitor population for the luminous red galaxies seen at $z \sim 3$ (although this conclusion depends upon the assumed duty cycle of the AGN). In contrast, the largest current redshift survey of the more numerous submillimetre-selected galaxy population (Chapman et al. 2005) identified no SMGs at $z \gtrsim 4$. As noted above, the need for precise locations for the SMGs from their μJy radio emission biased the redshift distribution to $z \lesssim 3.5$ (Chapman et al. 2005), and there could be a high-redshift tail (Dannerbauer et al. 2002, 2008; Wang et al. 2007; Younger et al. 2007; Greve et al. 2008; Wang, Barger & Cowie 2009; Knudsen et al. 2009). Pope et al. (2006) and Aretxaga et al. (2007) derived photometric redshift estimates (albeit much less precise than spectroscopic redshifts) for possible counterparts to SMGs and proposed that a relatively low fraction (< 10 per cent) of SMGs lie at $z \gtrsim 4$, suggesting that the Chapman et al. (2005) redshift distribution is representative of all SMGs. Nevertheless, there has been recent confirmation of three radio-identified SMGs lying at $z = 4$–4.5 (Daddi et al. 2008; Capak et al. 2008; Schinnerer et al. 2008), indicating that a tail of SMGs does exist at $z \gtrsim 4$.

In this paper we focus on a luminous SMG discovered in our deep 870-μm Large Apex BOlometer CAmera (LABOCA) Extended Chandra Deep Field South (ECDFS) Survey (LESS; PIs Smail, Walter & Weiss; Weiss et al. in preparation, hereafter W09) which is associated with a faint radio and mid-infrared source. Spectroscopic and photometric observations identify this source as an ultraluminous far-infrared galaxy at $z = 4.76$. This is currently the highest redshift SMG known, suggesting that intense star formation was occurring in galaxies when the Universe was just over 1 Gyr old.

We adopt cosmological parameters from the *WMAP* fits in Spergel et al. (2003): $\Omega_\Lambda = 0.73$, $\Omega_\mathrm{m} = 0.27$, and $H_0 = 71\,\mathrm{km\,s^{-1}\,Mpc^{-1}}$. At $z = 4.76$ the angular scale is $6.5\,\mathrm{kpc\,arcsec^{-1}}$, and the Universe is 1.3 Gyr old. All quoted magnitudes are on the AB system unless otherwise noted.

2 OBSERVATIONS AND SOURCE MULTIWAVELENGTH PROPERTIES

The full area of the ECDFS was mapped at $870\,\mu\mathrm{m}$ with LABOCA on the 12-m Atacama Pathfinder EXperiment (APEX; Güsten et al. 2006) telescope at Llano de Chajnantor in Chile as a joint ESO–Max Planck programme (the LESS collaboration). A total of 310 hrs of observing time (with 200 hrs of that on-source) was obtained which yielded a map covering the central $30' \times 30'$ of the field ($0.25\,\mathrm{deg}^2$) to an average rms of $\sim 1.2\,\mathrm{mJy}$. This is the largest contiguous deep submillimetre survey yet undertaken (c.f. the $\sim 0.25\,\mathrm{deg}^2$ 2-mJy rms SCUBA Half Degree Extragalactic Survey – SHADES; Coppin et al. 2006). The description of the observations, reduction and analysis of the map is given in W09. The robust catalogue derived from this map contains 121 SMGs at > 3.7-σ significance (chosen to provide an estimated false detection rate of ≤ 5 sources), and the multiwavelength identification and characterisation of the SMG population in the ECDFS will be presented in subsequent

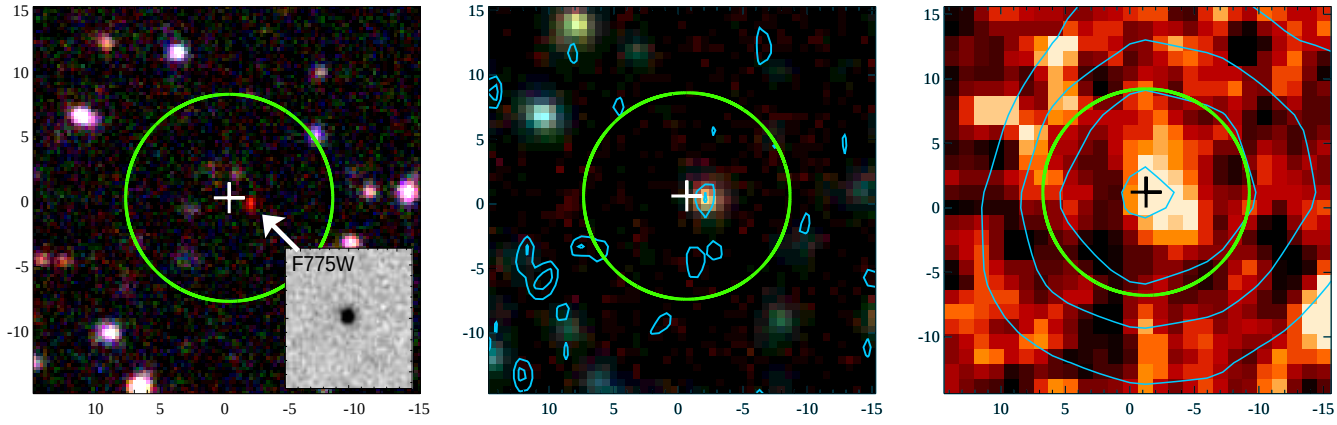

Figure 1. A selection of multiwavelength views of LESS J033229.4. The three panels show: (left) a true-colour ground-based BVR image of LESS J033229.4 from MUSYC, with a $2'' \times 2''$ inset illustrating the GOODS *HST* morphology in the F775W band (consistent with an unresolved point source); (centre) three-colour *Spitzer* 3.6, 4.5, 5.8 μm imaging from GOODS/SIMPLE with the Miller et al. (2008) VLA 1.4-GHz radio contours overlaid (starting at $2\,\sigma$ and increasing in steps of $1\,\sigma$); (right) the 24 μm imaging from the *Spitzer*–FIDEL survey with the LABOCA 870μm emission from W09 overlaid as contours (starting at $2\,\sigma$ and increasing in steps of $1\,\sigma$). The submillimetre position is indicated by a cross, and we also plot a circle representing the $8''$ search radius used to locate potential counterparts. We have robustly identified the SMG with a radio and 24-μm counterpart $\sim 1.5''$ away, which is coincident with a $z = 4.76$ galaxy (see text). Each panel is $15'' \times 15''$ in size and is orientated with North to the top and East to the left.

papers. Here we focus on the multiwavelength characteristics of a single source: LESS J033229.4−275619 (hereafter LESS J033229.4), detected at 870 μm with a flux density of 6.3 ± 1.2 mJy (S/N = 5.1) at $03^{\rm h}32^{\rm m}29.41^{\rm s}$ $-27°56'18.90''$ (J2000), with a 90 per cent positional uncertainty of $\sim 6''$ (W09). W09 apply a flux-deboosting algorithm to correct the raw flux and noise values for all of the LESS sources in order to obtain the most accurate submm photometry (see e.g. Coppin et al. 2005). In this paper we use the deboosted flux and noise of 5.0 ± 1.4 mJy for LESS J033229.4.

We use a new radio catalogue (Biggs et al. in preparation) which comprises emitters with peak flux densities in excess of $3\,\sigma$, where σ is determined locally, extracted from the Very Large Array (VLA) 1.4-GHz map of Miller et al. (2008). We search within $8''$ of the submm position for potential radio counterparts (see e.g. Downes et al. 1986; Ivison et al. 2002) and identify a single candidate at a radial distance of $1.5''$ with a flux density of $24.0 \pm 6.3\,\mu$Jy (S/N=3.8), assuming that it is a point source. The probability of this radio emitter being aligned by chance with the SMG is less than 2 per cent and we can assign this radio counterpart to the SMG with some confidence. Radio images suffer from similar flux boosting effects as the submm images and we thus adopt a deboosted 1.4-GHz flux density of $18.8 \pm 6.3\,\mu$Jy from Biggs et al. (in preparation), following extensive simulations of the kind described by Ibar et al. (2009). The positional accuracy of the radio data allows us to pinpoint LESS J033229.4 to $\alpha_{\rm J2000} = 03^{\rm h}32^{\rm m}29.30^{\rm s}$ $\delta_{\rm J2000} = -27°56'19.40''$ with an uncertainty of $\Delta\alpha = 0.2''$ and $\Delta\delta = 0.3''$ (see Ivison et al. 2007 and Fig. 1). Using this precise position for the robust radio counterpart of LESS J033229.4 we can now use the impressive archival observations of the ECDFS to derive its spectral energy distribution.

In the mid-to-far-infrared, a counterpart is detected at 3.6–8μm using the InfraRed Array Camera (IRAC; Fazio et al. 2004) data from the Great Observatories Origins Deep Survey (GOODS[1]; Dickinson, Giavalisco & the GOODS team 2003; Giavalisco et al. 2004) imaging of the central part of the ECDFS (GOODS-South) and in the wider area coverage provided by the *Spitzer* IRAC/MUSYC Public Legacy Survey in the ECDFS (SIMPLE[2]; Damen et al. in preparation). For the present analysis we use the 3-$''$ radius aperture photometry in the SIMPLE catalogue, as it provides close to optimal S/N for point sources, with the appropriate aperture corrections applied and corrected to total fluxes. In the mid-infrared, LESS J033229.4 is detected by the Far-Infrared Deep Extragalactic Legacy survey (FIDEL; Dickinson et al. in preparation) in the Multiband Imaging Photometer for *Spitzer* (MIPS; Rieke et al. 2004) 24 μm catalogue at $03^{\rm h}32^{\rm m}29.30^{\rm s}$ $-27°56'18.78''$, with a positional accuracy of 1–2$''$, given the FWHM and the source's S/N. The MIPS source lies within $0.6''$ of the radio counterpart and hence the radio and MIPS emission originate from the same source, given the combined error circle. We report a 24 μm flux density of $S_{24\mu{\rm m}} = 31.6 \pm 5.1\mu$Jy (S/N = 6.6), exploiting the deeper GOODS 24-μm imaging (Chary et al. in preparation). LESS J033229.4 is not detected at either 70 or 160 μm in the deep FIDEL imaging and so we adopt 3-σ upper limits at these wavelengths.

At shorter wavelengths, the region around LESS J033229.4 is covered by optical and near-infrared imaging from several ground and space-based public surveys: the Multiwavelength Survey by Yale–Chile (MUSYC[3]; Gawiser et al. 2006), the *Hubble Space Telescope (HST)* Advanced Camera for Surveys (ACS) Galaxy Evolution from Morphologies and SEDs survey (GEMS[4]; Rix et al.

[1] http://www.stsci.edu/science/goods/
[2] http://data.spitzer.caltech.edu/popular/SIMPLE
[3] http://www.astro.yale.edu/MUSYC
[4] http://www.mpia.de/GEMS/gems.htm

2004), and GOODS (Giavalisco et al. 2004; Giavalisco et al. in preparation). We list the fluxes or limits from these surveys in Table 1. The source is undetected in all bands shortward of $\sim 600\,$nm, although it is significantly detected in the redder wavebands, $V_{606}, R, i_{775}, z_{850}$. Unfortunately the source falls $\sim 1''$ outside the deep Very Large Telescope (VLT) Infrared Spectrometer And Array Camera (ISAAC) JHK imaging of GOODS-South and so there are currently only weak constraints on its near-infrared fluxes from MUSYC (Taylor et al. 2008).

Finally, turning to the X-ray waveband: from their analysis of the 1-Ms *Chandra* image, Giacconi et al. (2002) report the detection of an X-ray source at $03^{\rm h}32^{\rm m}29.44^{\rm s}$ $-27^\circ56''20.18''$ with a positional uncertainty of $2.1''$, with 0.5–2 and 2–10 keV fluxes of $(1.6 \pm 0.5) \times 10^{-16}$ and $< 7.6 \times 10^{-16}\,{\rm erg\,s^{-1}\,cm^{-2}}$, respectively. This position is consistent with the GOODS optical counterpart $0.8''$ away. However, this source (ID 618) is only listed in their supplementary catalogue and is based on a SExtractor (Bertin & Arnouts 1996) analysis of the X-ray image, for which the software was not intended. In contrast, no X-ray source is detected at this position in any of the analyses of the 250 ks, 1-, and 2-Ms images of the CDFS, by Lehmer et al. (2005), Alexander et al. (2003) or Luo et al. (2008), respectively. We thus extract 3-σ upper limits from the deepest 2-Ms *Chandra* imaging of Luo et al. (2008), corresponding to rest-frame 3–11.5 keV and 11.5—46 keV luminosity limits of $< 2.1 \times 10^{43}$ and $< 1.5 \times 10^{44}\,{\rm erg\,s^{-1}}$, respectively, which we use to constrain any contribution from an AGN to the bolometric luminosity (see § 3.2).

Table 1 summarises the fluxes or limits derived from the multiwavelength coverage of LESS J033229.4. From the optical photometry it is clear that the source is a V-band dropout. Assuming this arises from the presence of the Lyman limit in the V-band, this suggests a redshift of $z \approx 5$. The morphology of the source in the redder *HST* imaging is very compact, with an observed FWHM of $\lesssim 0.1''$ (or a half-light radius of $\lesssim 0.3\,$kpc), indicating that the source is unresolved (see inset in Fig. 1). Indeed, the source was photometrically and morphologically selected as a candidate $z = 3.5$–5.2 AGN by Fontanot et al. (2007). On this basis, LESS J033229.4 was observed with the FOcal Reducer and low dispersion Spectrograph (FORS2; Appenzeller et al. 1998) on the VLT by Vanzella et al. (2006) (see also Vanzella et al. 2008) as part of the ESO Large Programme 170.A-0788 (PI: Cesarsky). Their ID for this source is GDS J033229.29−275619.5 and they obtained a 4-hr exposure of it using the 300I grism, deriving a redshift of $z = 4.76$ on the basis of the identification of strong Lyα emission, N V and a continuum break (Fig. 2). The photometric properties of LESS J033229.4 are consistent with this claimed redshift, in particular the discontinuity at $\sim 600\,$nm is well reproduced by the Lyman limit at $z = 4.76$ (Fig. 3). This makes this source the highest redshift submillimetre-selected SMG yet discovered and indeed one of the highest redshift 24-μm-detected sources so far identified.

We obtained additional spectroscopic observations of LESS J033229.4 using the DEep Imaging Multi-Object Spectrograph (DEIMOS; Faber et al. 2003) on Keck on the nights of 2007 October 10 and 11. The total exposure time was 6.5 hrs in good conditions using the 600 lines mm^{-1} grating and the resulting spectrum (Fig. 2) shows contin-

Table 1. The observed photometry for LESS J033229.4 from *Chandra*, *HST*, MUSYC, *Spitzer*, APEX and the VLA. Note that we list the deboosted submm and radio fluxes, which is important in order to correctly model the SED and investigate the radio and submm properties of the SMG (see text). We use the *HST*-ACS photometry from Stark et al. (2007), which has already been corrected for the Lyα emission measured from the FORS2 rest-frame UV spectrum. We also give the 3.6 μm flux density, corrected down by 30 per cent to reflect the typical equivalent width of Hα in $z \sim 2$ SMGs (Swinbank et al. 2004; Takata et al. 2006). Where the source is undetected we quote a 3-σ upper limit to the flux density. Note: 1μJy is the equivalent of 23.9 AB magnitudes.

Filter /Wavelength	Flux Density (μ Jy)	Reference
0.5–8 keV	$< 3.7 \times 10^{-16}\,{\rm erg\,s^{-1}\,cm^{-2}}$	Luo et al. (2008)
0.5–2 keV	$< 8.5 \times 10^{-17}\,{\rm erg\,s^{-1}\,cm^{-2}}$	Luo et al. (2008)
2–8 keV	$< 6.3 \times 10^{-16}\,{\rm erg\,s^{-1}\,cm^{-2}}$	Luo et al. (2008)
U (352 nm)	< 0.087	Gawiser et al. (2006)
B_{435} (433 nm)	< 0.013	Fontanot et al. (2007)
B (461 nm)	< 0.039	Gawiser et al. (2006)
V (538 nm)	< 0.059	Gawiser et al. (2006)
V_{606} (597 nm)	0.072 ± 0.006	Stark et al. (2007)
R (652 nm)	0.215 ± 0.020	Gawiser et al. (2006)
i_{775} (771 nm)	0.350 ± 0.013	Stark et al. (2007)
z_{850} (905 nm)	0.405 ± 0.015	Stark et al. (2007)
J (1.2μm)	< 1.65	Taylor et al. (2008)
K (2.1μm)	< 3.20	Taylor et al. (2008)
3.6 μm	2.86 ± 0.06	Damen et al. in preparation
4.5 μm	4.04 ± 0.08	Damen et al. in preparation
5.8 μm	6.3 ± 0.4	Damen et al. in preparation
8.0 μm	9.2 ± 0.4	Damen et al. in preparation
24 μm	32 ± 5	Chary et al. in preparation
70 μm	< 2500	Dickinson et al. in preparation
160 μm	< 33000	Dickinson et al. in preparation
870 μm	5000 ± 1400	W09
20 cm	18.8 ± 6.3	Biggs et al. in preparation

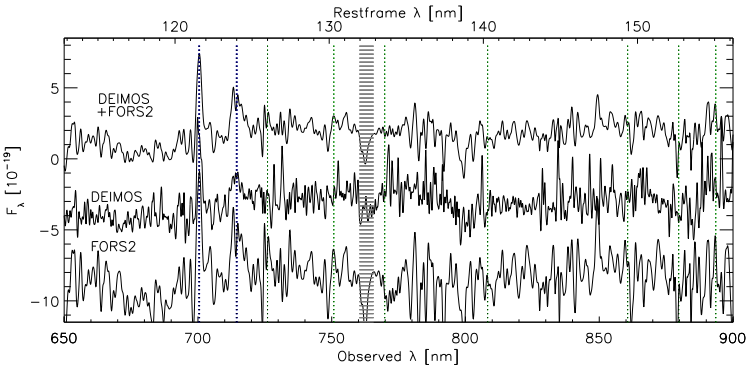

Figure 2. The optical spectrum of LESS J033229.4 derived from combining our new deep DEIMOS spectrum with the archival FORS2 spectrum from Vanzella et al. (2006). The upper spectrum is the combined dataset at the FORS2 resolution ($\sim$ 1.3 nm), while the lower spectra (arbitrarily offset in flux for clarity) show the individual DEIMOS spectrum convolved to $\sim$ 0.8 nm resolution and the FORS2 spectrum. The combined spectrum displays two strong emission lines and an associated continuum break. We identify the lines as Lyα and N V, yielding a redshift of $z \sim 4.76$. We mark these two emission features on the spectra and also indicate the expected wavelengths for other potential emission and absorption lines at the adopted redshift of $z = 4.76$: Si II 126.0, O I 130.3, C II 133.6, Si IV 140.3, Fe III 149.4, Si II 152.7 and C IV 155.1, as well as atmospheric absorption at 760 nm (shaded bar). The upper scale gives the rest-frame wavelength assuming a redshift of $z = 4.76$, and the flux scale is nominally in erg cm^{-2} s^{-1} Å^{-1}.

uum emission and the two strong emission lines seen in the FORS2 spectrum. We retrieved the reduced FORS2 spectrum of Vanzella et al. (2006) from the ESO archive and then convolved the DEIMOS spectrum to the ~ 1.3 nm resolution of the FORS2 spectrum before averaging the two spectra. The combined spectrum has an effective 10-m equivalent integration time of $\sim$ 9 hrs and is shown in Fig. 2. The combined spectrum displays a narrow Lyα emission line at 700.5 nm and a broad N V emission line at 714.5 nm with a width of $\sim$ 5 nm or $\sim$ 2000 km s^{-1} in the rest-frame and an integrated flux density comparable to Lyα ($\sim 1.4 \times 10^{-17}$ erg s^{-1} cm^{-2}). To search for weak broad lines we have convolved the spectrum to the FWHM of the N V line and find an emission feature corresponding to C IV 155.0 at very low significance, likely due to the strong telluric emission at these wavelengths. The spectral properties of the source, in particular the relatively strong and moderately broad N V, indicates the presence of an AGN, though the weak X-ray and 24 μm flux densities relative to the optical and far-infrared bands suggest a relatively weak AGN contribution to the bolometric luminosity.

High-redshift AGN are often associated with rest-frame far-infrared emission (e.g. Ivison et al. 2008), and as a final test of our identification of the SMG with this source, we can also ask what is the likelihood of finding such a high-redshift source close to the submillimetre position by chance. Using the AGN luminosity function from Fontanot et al. (2007), we calculate how many $z > 4$ AGN counterparts we would have expected to find at random given their volume density and the offset of the submillimetre source to the AGN, $\theta = 1.5''$. LESS J033229.4 has a rest-frame 145-nm luminosity of $M_{145} = -21.5$, calculated following Fan et al. (2000) and adopting $f_\nu \propto \nu^{-\alpha}$ with $\alpha = 0.5$. The volume density of AGN brighter than LESS J033229.4 is $\Phi(M_{145} < -21.5) \sim 2.6 \times 10^{-6}$ Mpc^{-3}, equivalent to a surface density $N \sim 34$ deg^{-2} for the integrated density at $z > 4$. The Poisson random probability of finding a $z > 4$ AGN at least as bright as ours is $P = 1 - \exp[-\pi\theta^2 N] \sim 10^{-5}$. Therefore it is extremely unlikely that our SMG is located within $1.5''$ of a high-redshift source by random chance, confirming the proposed association of the submillimetre emission with the $z = 4.76$ source.

3 RESULTS & ANALYSIS

3.1 Spectral Energy Distribution

The bright submillimetre flux density of LESS J033229.4 suggests that a massive burst of star formation is underway in this system at $z = 4.76$. To test if the observed radio and far-infrared emission is consistent with being produced by star formation, we calculate the radio-to-submm spectral index for LESS J033229.4, deriving $\alpha_{1.4}^{350} = 1.01 \pm 0.11$. This spectral index is in good agreement with the mean spectral index at $z = 4.76$ predicted from 17 local star-forming galaxies by Carilli & Yun (2000): $\alpha_{1.4}^{350} = 1.04 \pm 0.13$, as well as with local ULIRGs such as Arp 220, $\alpha_{1.4}^{350} \sim 1.09$. This confirms that the far-infrared–radio emission from LESS J033229.4 is consistent with massive star formation.

We therefore plot the multiwavelength spectral energy distribution (SED) of LESS J033229.4 in Fig. 3 and compare this to the SEDs of Arp 220 and M 82, normalised to match the observed $S_{870\,\mu m}$ of LESS J033229.4 – corresponding to rest-frame 150-μm emission, near the peak of the dust emission. This shows that while the Arp 220 and M 82 SEDs both fit the radio–far-infrared emission from LESS J033229.4, M 82 is significantly brighter in the mid-infrared, with only Arp 220 providing an adequate description of the SED across the rest-frame optical–to–radio. This confirms that this $z = 4.76$ SMG has an SED consistent with local star-formation-dominated ULIRGs, although we note that the rest-frame UV and 24 μm emission exceed that seen for Arp 220. Therefore we have also overplotted a redshifted composite QSO SED from the atlas of local, optically bright quasars compiled by Elvis et al. (1994), scaled to match our observed rest-frame UV photometry, in order to assess the likely bolometric contribution of an unobscured AGN to our observed SED (see Fig. 3). It is apparent from this simple exercise that any contribution from an unobscured AGN to the infrared luminosity of LESS J033229.4 is likely to be negligible, and we investigate this in detail in § 3.2.

From the scaled Arp 220 template, we calculate $L_{\rm FIR} = L_{(8-1000\,\mu m)} = 6.1 \times 10^{12}\,L_\odot$, a factor $\sim 5\times$ the bolometric luminosity of Arp 220 (Soifer et al. 1984; Sanders et al. 1988, 2003). We note that adopting the scaled M 82 template results in an $L_{\rm FIR}$ a factor of $\sim 1.5\times$ higher. Owing to the negative K correction in the submillimetre waveband, the bolometric luminosity of LESS J033229.4 is close to the median luminosity of the $z \sim 2$ population in Chapman et al. (2005) (see also Kovács et al. 2006; Coppin et al. 2008), even though its luminosity distance is $2.5\times$ larger.

Based on these SED arguments, which indicate that much of the far-infrared emission arises from star formation, we derive a SFR of $\sim 1000\,M_\odot\,{\rm yr}^{-1}$ for LESS J033229.4, following Kennicutt (1998) who assumes a burst lifetime of $\sim$ 100 Myr and a Salpeter (1955) initial mass function (IMF). Next, we estimate a dust mass of $M_{\rm d} \sim 5 \times 10^8\,M_\odot$ using the 870 μm flux density and the usual relation $S_{\nu_{\rm obs}} = B_{\nu'}(T)\kappa_{\nu'}\,M_{\rm d}\,(1+z)/D_{\rm L}^2$ (e.g. Hughes, Dunlop & Rawlings 1997), where $D_{\rm L}$ is the cosmological luminosity distance and $B_{\nu'}$ is the Planck function evaluated at the emitted frequency, $\nu' = \nu_{\rm obs}\,(1+z)$. We have extrapolated from an average wavelength-dependent mass-absorption coefficient of $\kappa_{125_{\mu m}} = 2.64\,{\rm m}^2\,{\rm kg}^{-1}$ assuming $\beta = 1.5$ (Dunne, Eales & Edmunds 2003). Based on the similar far-infrared luminosity and spectral properties of LESS J033229.4 to $z \sim 2$ SMGs we adopt the average gas/dust ratio for this population (~ 60; Greve et al. 2005; Tacconi et al. 2006; Kovács et al. 2006; Coppin et al. 2008), and so predict a gas mass for LESS J033229.4 of $\sim 3 \times 10^{10}\,M_\odot$. Comparing this mass to the SFR, we expect that LESS J033229.4 would consume its gas at its present SFR in $\sim$ 30–40 Myr. This predicted gas mass is similar to that determined for other $z > 4$ SMGs (Daddi et al. 2008; Schinnerer et al. 2008).

To place limits on the potential stellar mass of the galaxy, we now investigate if the rest-frame UV–optical emission can be fit by a stellar population using the HyperZ package (Bolzonella, Miralles & Pello 2000). We stress that this is a necessary, but not a sufficient, requirement to show that this emission actually arises from stars, rather than the AGN. We assume a solar metallicity stellar population model from Bruzual & Charlot (1993), a Calzetti et al. (2000) starburst attenuation law, and either a constant or

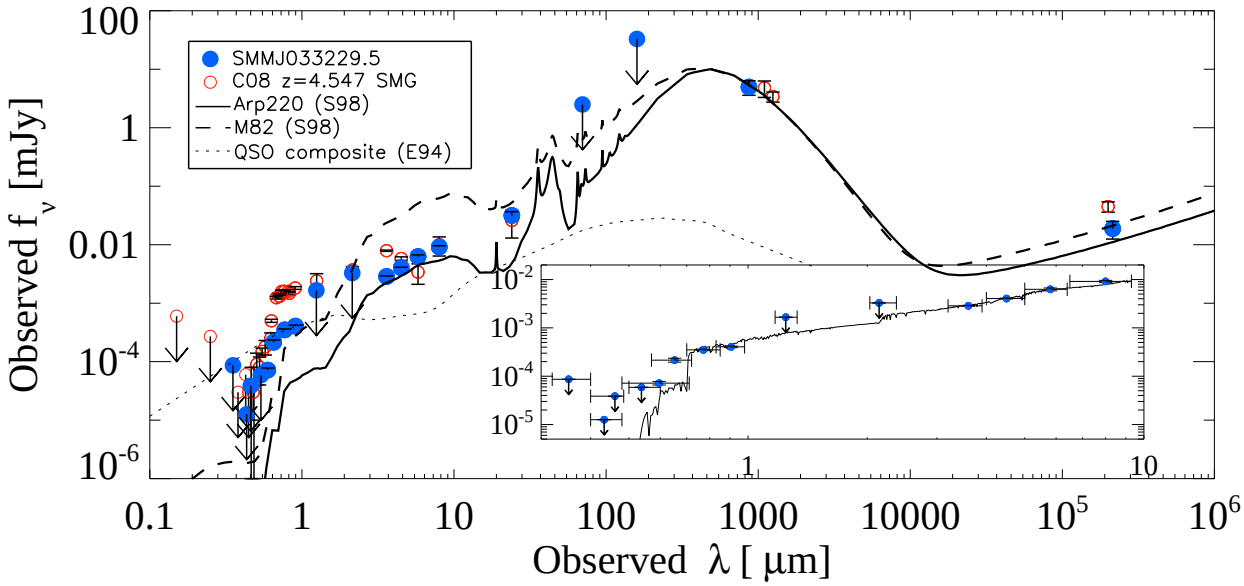

Figure 3. The SED of LESS J033229.4 showing the dominant and luminous rest-frame far-infrared emission indicating that the source is an ultraluminous infrared galaxy. For comparison we have overplotted the SED of Arp 220 and M 82 from Silva et al. (1998) redshifted to $z = 4.76$ and scaled to match the $S_{870\,\mu m}$ flux density of LESS J033229.4 and also a composite QSO SED from Elvis et al. (1994) redshifted to $z = 4.76$ scaled to match the rest-frame UV flux density. The good agreement with the starburst templates in the far-infrared and radio suggest that the bulk of the bolometric emission in this system arises from star formation. We also plot the SED of the $z = 4.5$ SMG SMM J100054.5+023436 from Capak et al. (2008; C08) to show the similar far-infrared properties, but the much more intense rest-frame UV emission from that system. The inset (in the same units as the larger plot) shows the best-fitting stellar SED from HyperZ to the optical–8 μm photometry, a 40-Myr old constant star formation model with moderate reddening, $A_V \sim 1.5$, which provides an acceptable fit of the rest-frame UV–optical emission in LESS J033229.4. However, we caution that the current SED can be equally well-fit by a power-law, as expected from a reddened AGN, leaving open the possibility that a significant fraction of the rest-frame near-infrared emission arises from the AGN.

single-burst star formation history. Under these assumptions, HyperZ shows that the observed SED can be fit by a stellar population at $z = 4.76$, although statistically a reddened power-law provides as good a fit. The best-fit SED is a 40-Myr old constant star formation model with moderate reddening, $A_V \sim 1.5$ (see inset Fig. 3). However, the absence of useful limits on the galaxy's SED in the observed JHK bands, sampling the critical region around the Balmer and 4000Å breaks, means that there is significant uncertainty in these parameters, with statistically acceptable solutions with ages up to $\gtrsim 500$ Myr and lower reddening, $A_V \lesssim 0.5$. Even this range of fits should be used with caution as the potentially dominant contribution from the AGN, as well as the complex mix of dust and stars, in this SMG will mean that the luminosity-weighted ages and reddening will vary strongly with wavelength as different regions within the galaxy are probed. Hence, in the following we simply assume a canonical duration of the SMG-phase of ~ 100 Myr (Swinbank et al. 2006), and focus on the rest-frame near-infrared luminosity which should suffer the least AGN contamination and provide the most robust estimate of the stellar mass of the galaxy.

From a simple interpolation of the SED we derive a rest-frame K-band luminosity of $M_K \sim -24.0$ or $L_K \sim 5 \times 10^{11}\,L_\odot$. To estimate a limit on the stellar mass from this we use the parameterisation for $L_K/M_\odot$ for a constant star formation model from Borys et al. (2005). For star formation which has been occuring for 100 Myr this gives $L_K/M_\star \sim 10$ (40- and 300-Myr durations correspond to $L_K/M_\odot \sim 50$ and 7), implying a typical stellar mass of $M\star \lesssim 5 \times 10^{10}\,M_\odot$. This has an uncertainty of at least a factor of 3–5×, even before considering the potential contribution from an AGN to the rest-frame near-infrared emission. Nevertheless, we note that this limit on the stellar mass is comparable to the predicted gas mass of the system and that for ages of ~ 100 Myr, the stellar mass produced in the burst implies a SFR of $\sim 500\,M_\odot\,yr^{-1}$, similar to that derived from the far-infrared. In contrast, Stark et al. (2007) estimate a stellar mass for LESS J033229.4 of $M_\star \sim 1.3 \times 10^{11}\,M_\odot$, assuming the mass-to-light ratio appropriate for a $\sim$ 1-Gyr old stellar population, which is unlikely to be valid for a system with a current SFR of $\sim 1000\,M_\odot\,yr^{-1}$.

3.2 Constraints on AGN energetics

The rest-frame UV compact morphology (FWHM of $\lesssim 0.1''$; or a half-light radius of $\lesssim 0.3$ kpc) and spectroscopy of LESS J033229.4 indicate that it hosts an AGN. For comparison, about ~ 10 per cent of $z \sim 2$ SMGs are classed as 'compact', with half-light radii of < 0.6 kpc (Swinbank et al. 2009). Similar spectral signatures of AGN emission are also seen in the rest-frame UV spectra of around 25 per cent of the radio-detected SMG population at $z \sim 2$–3 (Chapman et al. 2005), suggesting a mix of star formation

and AGN in the galaxy. In particular, LESS J033229.4's spectral properties are very similar to the first spectroscopically identified SMG: the type-2 or narrow-line QSO SMM J02399−0136 at $z = 2.803$ (Ivison et al. 1998a). SMM J02399−0136 also shows strong Lyα and a comparably bright and broad N V line, with a width of $1800\,\mathrm{km\,s^{-1}}$. Although the emission lines in SMM J02399−0136 are proportionally stronger relative to the continuum and the source is intrinsically more luminous than LESS J033229.4.

We can use the strength of the N V emission and other SED constraints to estimate the potential luminosity of the AGN component in LESS J033229.4 and compare these to our X-ray limits, where we are confident that any AGN emission will dominate. Using the observed 2–8 keV limit (rest-frame 11.5–46 keV) and assuming $\Gamma = 2.0$ we derive a conservative limit on the rest-frame 2–10 keV luminosity of $< 1.7 \times 10^{44}\,\mathrm{erg\,s^{-1}}$. This will be almost unaffected by the presence of absorption assuming absorbing column densities of $N_\mathrm{H} \lesssim 10^{25}\,\mathrm{cm^{-2}}$, i.e. not heavily Compton thick. A more sensitive limit comes from the observed 0.5–2 keV limit which yields a rest-frame 2–10 keV luminosity limit of $< 2.5 \times 10^{43}\,\mathrm{erg\,s^{-1}}$. However, this is also more sensitive to the assumed absorption in the system and so we will use our more conservative limit in the following.

Starting from the measured N V emission-line luminosity of $\sim 3 \times 10^{42}\,\mathrm{erg\,s^{-1}}$, we can use the observed N V–X-ray luminosity ratio found for SMM J02399−0136 (Ivison et al. 1998a; Bautz et al. 2000) to predict the rest-frame 2–10 keV luminosity of LESS J033229.4 of $\sim 1 \times 10^{44}\,\mathrm{erg\,s^{-1}}$. We can also attempt to estimate the luminosity of the AGN using the 24 μm flux density under the extreme assumption that the 24 μm emission is entirely due to the AGN. Using the derived rest-frame 6 μm luminosity of $1.2 \times 10^{45}\,\mathrm{erg\,s^{-1}}$ we estimate a rest-frame 2–10 keV luminosity of $\approx 3 \times 10^{44}\,\mathrm{erg\,s^{-1}}$ based on Alexander et al. (2008). Similarly, assuming that the UV continuum luminosity of LESS J033229.4 is dominated by emission from the AGN, we can predict the AGN luminosity. We take the observed rest-frame 145-nm absolute magnitude ($M_{145} = -21.5$) and convert this to rest-frame 250-nm assuming $\alpha = -0.44$ ($S_\nu \propto \nu^\alpha$; Vanden Berk et al. 2001). We then use the α_ox relationship of Steffen et al. (2006) and convert between different X-ray bands assuming $\Gamma = 2.0$, to derive a rest-frame 2–10 keV luminosity of $5 \times 10^{43}\,\mathrm{erg\,s^{-1}}$.

These three estimates are in the range 0.5–3 $\times$ $10^{44}\,\mathrm{erg\,s^{-1}}$ and so are consistent with our observed X-ray limit, given the significant uncertainties in the calculations.

4 DISCUSSION

Our estimates of the stellar and gas masses of LESS J033229.4 in § 3.1 are both crude and highly uncertain; nevertheless, both masses are comparable to those derived for the better-constrained and similarly bolometrically luminous $z \sim 2$ SMG population. The implied baryonic mass of the galaxy is thus likely to be $\sim 10^{11}\,\mathrm{M_\odot}$, suggesting that the ultraluminous starburst is occuring in a massive galaxy. Indeed, similar constraints on the host galaxy masses have been derived for the other examples of $z > 4$ SMGs (e.g. Daddi et al. 2008; Schinnerer et al. 2008).

Our three predictions of the X-ray luminosity of the AGN in § 3.2 suggest the luminosity of the AGN in LESS J033229.4 is $\sim 10^{44}\,\mathrm{erg\,s^{-1}}$ and that the AGN may dominate the emission in the X-ray and UV, while making a modest contribution to the mid-infrared luminosity. Using the X-ray–to–infrared luminosity ratio for local AGN (e.g. Alexander et al. 2005) we expect that the AGN contributes $\lesssim 20$ per cent of the bolometric luminosity and hence the bulk of the bolometric luminosity of LESS J033229.4 arises from star formation.

The discovery of LESS J033229.4 at $z = 4.76$ and three $z = 4$–4.5 SMGs from Capak et al. (2008) and Daddi et al. (2008) indicates that galaxies with SFRs of $\sim 1000\,\mathrm{M_\odot\,yr^{-1}}$ are present at high redshifts. Using these four $z > 4$ SMGs, and the areas of the surveys they were derived from, we can place a lower limit on the surface density of SMGs at these redshifts of $\gtrsim 6\,\mathrm{deg^{-2}}$, or a volume density of $\gtrsim 1.5 \times 10^{-7}\,\mathrm{Mpc^{-3}}$ conservatively assuming the surveys are uniformly sensitive across $z = 4$–8. Note that if we include the likely $z > 4$ SMG from Wang et al. (2007) (see also Wang, Barger & Cowie 2009), then these limits increase by ~ 15 per cent.

To test whether these high-redshift SMGs can evolve into luminous red galaxies at $z \sim 3$, we compute the expected fading of LESS J033229.4 from $z \sim 4.5$ to $z \sim 3$. Qualitatively, the inferred SFRs of the four $z > 4$ SMGs ($\sim 10^3\,\mathrm{M_\odot\,yr^{-1}}$), with estimated duration of order 100 Myr, are sufficient to form $> 10^{11}\,\mathrm{M_\odot}$ of stellar mass needed to match the properties of luminous red galaxies seen at $z \sim 3$, and there is enough time between $z \sim 4$ and $z \sim 3$ to age their stellar populations sufficiently. To quantitatively confirm this we adopt an approach that, while uncertain, is insensitive to the AGN contribution to the rest-frame K-band luminosity of LESS J033229.4. We assume a constant star formation rate at the observed level of $1000\,\mathrm{M_\odot\,yr^{-1}}$ for 100 Myr and that the starburst is observed half way through, then we estimate fading after $\sim$ 1–1.5 Gyr of $\Delta K \sim 1.1$–1.3 in the rest-frame K-band resulting in a typical SMG-descendent at $z \sim 3$ with $M_K \sim -24.7 \pm 0.1$ and observed colours of $(J - K) \sim 0.6$–0.9, assuming Bruzual & Charlot (1993) stellar models. Using the Maraston (1998) stellar population models these predictions become $\Delta K \sim 0.7$–1.7, $M_K \sim -24.7 \pm 0.5$ and $(J - K) \sim 1.0$–1.3. These predicted luminosities and colours are in reasonable agreement with those of the reddest luminous galaxies at $z \sim 2.5$–3.5, which have $M_K \lesssim -23.5 \pm 0.5$ and $(J - K) \geq 1.3$ (e.g. Marchesini et al. 2009).

We can also ask whether the space densities of these two populations are consistent with this evolutionary cycle. Our lower limit on the space density of SMGs at $z \sim 4$–8 is $\gtrsim 1.5 \times 10^{-7}\,\mathrm{Mpc^{-3}}$, so correcting for the duty cycle assuming a 100-Myr lifetime ($\sim 9\times$) this suggests that there will be $\gtrsim 10^{-6}\,\mathrm{Mpc^{-3}}$ descendents at $z \sim 2.5$–3.5. This compares to the measured space density of luminous galaxies at these redshifts of $\sim 5 \times 10^{-5}\,\mathrm{Mpc^{-3}}$ of which $\sim$ 20–30 per cent have red colours (Marchesini et al. 2007; Marchesini et al. 2009), or $\sim 10^{-5}\,\mathrm{Mpc^{-3}}$. This suggests that we have so far only detected ~ 10 per cent of the SMG progenitors at $z > 4$ of the $z \sim 3$ evolved luminous galaxies if all of the latter have a previous ultraluminous phase (c.f. Stark et al. 2009), or alternatively that there should be a surface density of $\sim 100\,\mathrm{deg^{-2}}$ SMGs at $z > 4$, corresponding to ~ 10 per cent of the $\gtrsim 5\,\mathrm{mJy}$ SMG population.

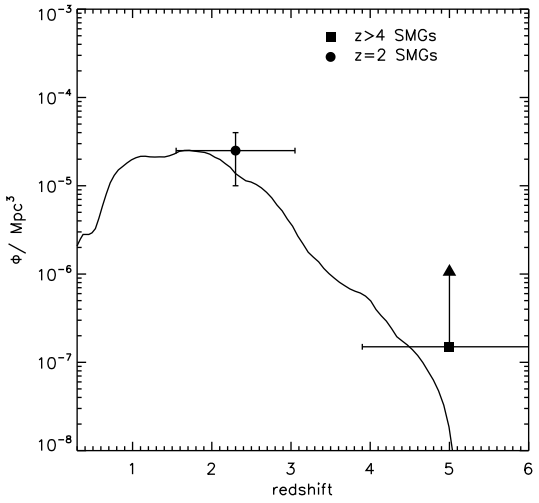

Figure 4. A comparison of the volume density of radio-detected SMGs with $S_{1.4\,\mathrm{GHz}} > 30\,\mu$Jy and $S_{850\,\mu\mathrm{m}} > 5\,$mJy from the GALFORM model of Baugh et al. (2005) to our limit on the volume density of $z > 4$ SMGs and the measured density of $z \sim 2$ SMGs from Chapman et al. (2005). This demonstrates that these detailed theoretical models are just consistent with these current observations, and so the discovery of more examples of $z > 4$ SMGs within the ECDFS would result in a disagreement with the model predictions.

More detailed theoretical galaxy formation models have achieved a rough agreement with the number counts and the median redshift of the SMG population (e.g. Baugh et al. 2005; Swinbank et al. 2008). The Baugh et al. (2005) semi-analytical galaxy formation model implements a top-heavy IMF in bursts in order to reproduce the submillimetre number counts and has been shown by Swinbank et al. (2008) to provide a reasonable description of the far-infrared properties of submillimetre galaxies at $z \sim 2$. We now investigate if the proportion of spectroscopically-confirmed high-redshift SMGs can provide a more stringent test of this model. In Fig. 4 we compare the volume densities of spectroscopically-confirmed SMGs to the model predictions (Baugh et al. 2005). Baugh et al. (2005) predict surface and volume densities of $\gtrsim 7\,\mathrm{deg}^{-2}$ and $\gtrsim 2\times10^{-7}\,\mathrm{Mpc}^{-3}$ (for $z \sim 4$–8), respectively, for SMGs with $S_{850\,\mu\mathrm{m}} > 5\,$mJy (see Swinbank et al. 2008). Imposing a radio-detection constraint ($\gtrsim 30\,\mu$Jy), which can be directly compared against the SMG samples with spectroscopic confirmation, reduces these predictions by a factor of ~ 2 (Fig. 4). Both of these estimates are consistent with our current limits on the volume densities of SMGs at $z > 4$ (as well as the measured volume density at $z \sim 2$ from Chapman et al. 2005). However, we note that the follow-up of the LABOCA survey of the ECDFS has only just begun and so it is possible that more $z > 4$ SMGs will be uncovered. Hence, we suggest that it is probable that the current semi-analytic models underpredict the numbers of very high redshift ULIRGs. In particular, if an example of a $z > 5$ SMG is found in existing submillimetre surveys then this will place strong constraints on these models.

5 CONCLUSIONS

LESS J033229.4 is currently the highest redshift submillimetre-selected galaxy known. At $z = 4.76$, it is seen just over 1 Gyr after the Big Bang, yet it has similar properties to the SMG population seen at the peak of their activity at $z \sim 2$ when the Universe was nearly 3× older. The SED and rest-frame UV spectrum indicate that LESS J033229.4 is a composite AGN/starburst galaxy caught in a phase where star formation ($\mathrm{SFR} \sim 1000\,\mathrm{M}_\odot\,\mathrm{yr}^{-1}$) is dominating the bolometric emission.

At $z = 4.76$, 870 μm samples near the SED peak, providing a good constraint on the far-infrared luminosity of SMG of $6 \times 10^{12}\,\mathrm{L}_\odot$. But in order to accurately determine the SED peak shape and bulk dust temperature of LESS J033229.4 one requires photometry on the Wien side of the peak of the SED from observations of the ECDFS at 250, 350 or 500 μm with the *Herschel Space Observatory* or the Balloon-borne Large Aperture Submillimetre Telescope (BLAST; Pascale et al. 2008). Our preferred Arp 220-like SED fit predicts 250, 350 and 500 μm flux densities of ~ 5, 9, and 10 mJy at these wavelengths, which are likely to prove to be challenging for either *Herschel* or BLAST due to confusion. Although a deep 350 μm (rest-frame 60μm) or 450μm flux density measurement would be feasible with future APEX measurements using the SABOCA submillimetre camera or the James Clerk Maxwell Telescope's Submillimetre Common-User Bolometer Array 2 (SCUBA-2), respectively.

Based on our estimated dust mass of $5 \times 10^8\,\mathrm{M}_\odot$ and adopting a $z \sim 2$ SMG average gas/dust ratio, we predict a gas mass of $3 \times 10^{10}\,\mathrm{M}_\odot$, similar to that measured for other $z > 4$ SMGs (Daddi et al. 2008; Schinnerer et al. 2008). At $z = 4.76$ ^{12}CO(5–4) emission should be detectable using current interferometric facilities. The confirmation of a massive reservoir of gas in LESS J033229.4 would enable the study of the gas and dynamics of galaxy formation in detail when the Universe was only 1 Gyr old, and so better place LESS J033229.4 in context with SMGs and red luminous galaxies at $z \sim 3$.

As with the original identification of SMGs (Ivison et al. 1998a), it is likely that selection effects may be strongly influencing our view of the properties of the very high-redshift SMG population. We note that if LESS J033229.4 had not been identified as a compact, potential high-redshift, AGN then it would not have been spectroscopically observed and if it had not shown strong line emission (at least in part from the AGN) then a redshift would never have been measured. Similarly, the morphologically complex optical counterpart of the Capak et al. (2008) SMG was first identified as a weak radio source associated with a potentially $z > 4$ V-band dropout object, and the redshifts for the two $z = 4.05$ Daddi et al. (2008) SMGs were obtained from the serendipitous detection of redshifted ^{12}CO(4–3) emission in observations of an unrelated nearby $z = 1.5$ BzK galaxy. A complete view of the properties of the $z > 4$ SMG population will require a concerted identification programme and multiwavelength follow-up, but not withstanding this, at present we can conclude that there appears to be an similarly diverse population of intense star-bursting galaxies at $z \gtrsim 4$ as there is at $z \sim 2$.

Assuming that red luminous galaxies at $z \sim 3$ are all

descendants of $z = 4$–8 SMGs we estimate the space density of the SMG progenitor population would be of the order of $\sim 10^{-5}\,\mathrm{Mpc}^{-3}$ at $z \sim 4$–8, assuming a 100-Myr lifetime for the ULIRG-phase, corresponding to a surface density of ~ 50–$100\,\mathrm{deg}^{-2}$. Current observational limits on the $z > 4$ SMG population are thus consistent with them being the progenitors of $> 10\%$ of the passive massive galaxy population at $z \sim 3$. These limits are in agreement with the semi-analytical model predictions for radio-detected SMGs at these redshifts. However, we note that if further follow-up shows that the surface density of SMGs at $z \sim 4$–8 is closer to the $\sim 100\,\mathrm{deg}^{-2}$ necessary for them to form all of the red luminous galaxy population at $z \sim 3$, then the models will be underpredicting the number of SMGs at $z > 4$ by about a order of magnitude. Alternatively, many $z \sim 3$ red luminous galaxies may form without a superluminous phase. Either way, statistically significant samples of SMGs need to be studied and followed up with spectroscopy in fields with extensive multiwavelength coverage before we will be able to determine true predominance and role of SMGs at $z > 4$. The panoramic and deep Cosmology Legacy Surveys planned with SCUBA-2 will obtain the tens of thousands of SMGs needed to begin the search in earnest for SMGs at even higher redshifts, $z \gg 4$–8.

6 ACKNOWLEDGMENTS

We would like to thank an anonymous referee for helpful comments and suggestions on the paper. We thank John Helly for help with extracting information from the Millenium and GALFORM databases. KEKC acknowledges support from a Science and Technology Facilities Council (STFC) fellowship. IRS, DMA and JSD acknowledge support from the Royal Society. JEG and JLW acknowledge support from the STFC, and AMS acknowledges support from a Lockyer fellowship. The work of DS was carried out at Jet Propulsion Laboratory (JPL), California Institute of Technology (Caltech), under a contract with National Aeronautics and Space Administration (NASA). WNB acknowledges support from the *Chandra* X-ray Observatory's grant SP8-9003A.

Observations have been carried out using APEX and the VLT under Program IDs: 080.A-3023, 079.F-9500, 170.A-0788, 074.A-0709, and 275.A-5060. APEX is operated by the Max-Planck-Institut für Radioastronomie, the European Southern Observatory, and the Onsala Space Observatory. We would like to thank the staff for their aid in carrying out the observations. Some of the data presented herein were obtained at the W. M. Keck Observatory, which is operated as a scientific partnership among Caltech, the University of California and NASA. The Keck Observatory was made possible by the generous financial support of the W. M. Keck Foundation. This work is based in part on observations from the Legacy Science Program, made with the *Spitzer Space Telescope*, which is operated by JPL, Caltech under a contract with NASA; and support for this work was provided by NASA through an award issued by JPL/Caltech. This research has also made use of the NASA/IPAC Extragalactic Database (NED) which is operated by JPL/Caltech, under contract with NASA. Ned Wright's Javascript Cosmology Calculator was also used in preparing this paper (Wright et al. 2006).

REFERENCES

Alexander D.M. et al., 2003, AJ, 126, 539
Alexander D.M., Bauer F.E., Chapman S.C., Smail I., Blain A.W., Brandt W.N., Ivison R.J., 2005, ApJ, 632, 736
Alexander D.M. et al., 2008, ApJ, 687, 835
Appenzeller I. et al., 1998, The Messenger, 94, 1
Archibald E.N., Dunlop J.S., Hughes D.H., Rawlings S., Eales S.A., Ivison R.J., 2001, MNRAS, 323, 417
Aretxaga I. et al., 2007, MNRAS, 379, 1571
Baugh C.M., Lacey C.G., Frenk C.S., Granato G.L., Silva L., Bressan A., Benson A.J., Cole S., 2005, MNRAS, 356, 1191
Bautz M.W., Malm M.R., Baganoff F.K., Ricker G.R., Canizares C.R., Brandt W.N., Hornschemeier A.E., Garmire G.P., 2000, ApJ, 543, L119
Bertin E., Arnouts S., 1996, A&AS, 117, 393
Blain A.W., Smail I., Ivison R.J., Kneib J.-P., Frayer D.T., 2002, Phys. Rep., 369, 111
Bolzonella M., Miralles J.-M., Pello R., 2000, A&A, 363, 476
Borys C., Smail I., Chapman S.C., Blain A.W., Alexander D.M., Ivison R.J., 2005, ApJ, 635, 853
Bower R.G., Benson A.J., Malbon R., Helly J.C., Frenk C.S., Baugh C.M., Cole S., Lacey C.G., 2006, MNRAS, 370, 645
Bruzual G., Charlot S., 1993, ApJ, 405, 538
Calzetti D., Armus L., Bohlin R.C., Kinney A.L., Koornneef J., Storchi-Bergmann T., 2000, ApJ, 533, 682
Capak P. et al., 2008, ApJ, 681, L53
Carilli C.L., Yun M., 2000, ApJ, 530, 618
Carilli C.L., et al., 2000, ApJ, 533, 13
Carilli C.L., et al., 2001, ApJ, 555, 625
Chapman S.C., Blain A.W., Smail I., Ivison R.J., 2005, ApJ, 622, 772
Cimatti A. et al., 2004, Nat., 430, 184
Cimatti A. et al., 2008, A&A, 482, 212
Condon J.J., 1992, ARA&A, 30, 575
Coppin K. et al., 2005, MNRAS, 357, 1022
Coppin K. et al., 2006, MNRAS, 372, 1621
Coppin K. et al., 2008, MNRAS, 384, 1597
Daddi E. et al., 2005, ApJ, 626, 680
Daddi E. et al., 2008, ApJ, arXiv:0810.3108
Dannerbauer H., Lehnert M., Lutz D., Tacconi L., Bertoldi F., Carilli C., Genzel R., Menten K., 2002, ApJ, 573, 473
Dannerbauer H., Walter F., Morrison G., 2008, ApJ, 673, L127
Dickinson M., Giavalisco M., & the GOODS team, 2003, in "The Mass of Galaxies at Low and High Redshift", eds. R. Bender & A. Renzini, Springer-Verlag, 324
Downes A.J.B., Peacock J.A., Savage A., Carrie D.R., 1986, MNRAS, 218, 31
Downes D. et al., 1999, A&A, 347, 809
Dunne L., Eales S., Edmunds M., 2003, MNRAS, 341, 589
Elvis M. et al., 1994, ApJS, 95, 1
Faber S.M. et al., Proc. SPIE, 4841, 1657
Fan X. et al., 2000, AJ, 119, 1
Fazio G.G. et al., 2004, ApJS, 154, 10

Fontanot F., et al., 2007, A&A, 461, 39
Gawiser E., et al., 2006, ApJS, 162, 1
Gear W.K., Lilly S.J., Stevens J.A., Clements D.L., Webb T.M., Eales S.A., Dunne L., 2000, MNRAS, 316, 51L
Giacconi R. et al., 2002, ApJS, 139, 369
Giavalisco M., et al., 2004, ApJ, 600, L93
Granato G., et al., 2004, ApJ, 600, 580
Greve T.R., et al., 2005, MNRAS, 359, 1165
Greve T.R., Pope A., Scott D., Ivison R.J., Borys C., Conselice C.J., Bertoldi F., 2008, MNRAS, 389, 1489
Güsten R., Nyman L.A., Schilke P., Menten K., Cesarsky C., Booth R., 2006, A&A, 454, L13
Hartley W.G., et al., 2008, MNRAS, 391, 1301
Helou G., Bicay M.D., 1993, ApJ, 415, 93
Hopkins P.F., Hernquist L., Cox T.J., Di Matteo T., Martini P., Robertson B., Springel V., 2005, ApJ, 630, 705
Hughes D.H., Dunlop J.S., Rawlings S., 1997, MNRAS, 289, 766
Ibar E., Ivison R.J., Biggs A., Vir Lal D., Best P.N., Green D.A., 2009, MNRAS, submitted
Ivison R.J., et al., 1998a, MNRAS, 298, 583
Ivison R.J., et al., 1998b, ApJ, 494, 211
Ivison R.J., et al., 2002, MNRAS, 337, 1
Ivison R.J., et al., 2004, ApJS, 154, 124
Ivison R.J., et al., 2007, MNRAS, 380, 199
Ivison R.J., et al., 2008, MNRAS, 390, 1117
Kennicutt R.C., 1998, ARA&A, 36, 189
Kong X., et al., 2006, ApJ, 638, 189
Knudsen K.K. et al., 2009, A&A, arXiv:0812.3409
Kovács A., Chapman S.C., Dowell C.D., Blain A.W., Ivison R.J., Smail I., Phillips T.G., 2006, ApJ, 650, 592
Lehmer B.D., et al., 2005, ApJS, 161, 21
Luo B., et al., 2008, ApJS, 179, 19
Maraston C., 1998, MNRAS, 300, 872
Marchesini D., et al., 2007, ApJ, 656, 42
Marchesini D., van Dokkum P.G., Forster-Schreiber N.M., Franx M., Labbe I., Wuyts S., 2009, ApJ, arXiv:0811.1773
McGrath E.J., Stockton A., Canalizo G., 2007, ApJ, 669, 241
McMahon R.G., Omont A., Bergeron J., Kreysa E., Haslam C.G.T., 1994, MNRAS, 267, L9
Miller N. et al., 2008, ApJS, 179, 114
Omont A., McMahon R.G., Cox P., Kreysa E., Bergeron J., Pajot F., Storrie-Lombardi L.J., 1996, A&A, 315, 1
Pascale E. et al., 2008, ApJ, 681, 400
Pope A. et al., 2006, MNRAS, 370, 1185
Priddey R.S., Ivison R.J., Isaak K.G., 2008, MNRAS, 383, 289
Rieke G.H. et al., 2004, ApJS, 154, 25
Rix H.-W. et al., 2004, ApJS, 152, 163
Salpeter E.E., 1955, ApJ, 121, 161
Sanders D.B., Soifer B.T., Elias J.H., Neugebauer G., Matthews K., 1988, ApJ, 328, L35
Sanders D.B., Mazzarella J.M., Kim D.C., Surace J.A., Soifer B.T., 2003, AJ, 126, 1607
Schinnerer E., et al., 2008, ApJ, 689, 5L
Silva L., Granato G.L., Bressan A., Danese L., 1998, ApJ, 509, 103
Soifer B.T. et al., 1984, ApJ, 283, L1
Stark D.P., Bunker A.J., Ellis R.S., Eyles L.P., Lacy M., 2007, ApJ, 659, 84
Stark D.P., Ellis R.S., Bunker A.J., Bundy K., Targett T., Benson A., Lacy M., 2009, ApJ, arXiv:0902.2907
Steffen A.T., Strateva I., Brandt W.N., Alexander D.M., Koekemoer A.M., Lehmer B.D., Schneider D.P., Vignali C., 2006, AJ, 131, 2826
Stockton A., et al., 2008, ApJ, 672, 146
Spergel D.N. et al., 2003, ApJS, 148, 175
Swinbank A.M., Smail I., Chapman S.C., Blain A.W., Ivison R.J., Keel W.C., 2004, ApJ, 617, 64
Swinbank A.M., Chapman S.C., Smail I., Lindner C., Borys C., Blain A.W., Ivison R.J., Lewis G.F., 2006, MNRAS, 371, 465
Swinbank A.M., et al., 2008, MNRAS, 391, 420
Swinbank A.M., et al., 2009, to be submitted
Taylor E.N., et al., 2008, ApJS, submitted
Tacconi L.J. et al., 2006, ApJ, 640, 228
Takata T., Sekiguchi K., Smail I., Chapman S.C., Geach J.E., Swinbank A.M., Blain A., Ivison R.J., 2006, ApJ, 651, 713
Vanden Berk D.E. et al., 2001, AJ, 122, 549
Vanzella E. et al., 2006, A&A, 454, 423
Vanzella E. et al., 2008, A&A, 478, 83
Wang W.-H., Cowie L.L., van Saders J., Barger A.J., Williams J.P., 2007, ApJ, 670, L89
Wang W.-H., Barger A.J., Cowie L.L., 2009, ApJ, 690, 319
Wright E.L., 2006, PASP, 118, 1711
Younger J. D. et al., 2007, ApJ, 671, 1531
Younger J. D. et al., 2008, MNRAS, 387, 707